

# High propagating velocity of spin waves and temperature dependent damping in a CoFeB thin film

Haiming Yu,<sup>a),b)</sup> R. Huber,<sup>a)</sup> T. Schwarze, F. Brandl, T. Rapp, P. Berberich, G. Duerr, and D. Grundler<sup>c)</sup>

*Lehrstuhl für Physik funktionaler Schichtsysteme, Technische Universität München, Physik Department, James-Frank-Str. 1, D-85747 Garching b. München, Germany*

(Received 24 April 2012; accepted 9 June 2012; published online 29 June 2012)

Spin wave propagation in a magnetron-sputtered CoFeB thin film is investigated. We apply both in-plane and out-of-plane magnetic fields. At room temperature, we find velocities of up to 25 and 3.5 km/s, respectively. These values are much larger compared to a thin permalloy film. Analyzing the resonance linewidth, we obtain an intrinsic Gilbert damping parameter of about 0.007 at room temperature. It increases to 0.023 at 5 K. CoFeB is a promising material for magnonic devices supporting fast propagating spin waves. © 2012 American Institute of Physics.

[<http://dx.doi.org/10.1063/1.4731273>]

The alloy CoFeB is used in magnetic tunnel junctions (MTJs), which form the basis for magnetic random access memory (MRAM), read heads in hard disk drives, as well as spin-logic based devices.<sup>1–3</sup> At the same time, CoFeB films have been relevant to explore photo-induced spin-wave excitations in magnetic antidot lattices.<sup>4</sup> Ferromagnetic resonance measurements evidenced a small linewidth for CoFeB.<sup>5–10</sup> For magnonic applications,<sup>11,12</sup> electrically generated spin waves would be very interesting. Spin-transfer torque (STT) which is found to occur in dc-current biased CoFeB-based MTJs (Ref. 13) has been shown to excite spin dynamics.<sup>14,15</sup> It has been predicted that the excitation of propagating spin waves by STT depends, however, crucially on the out-of-plane component of the magnetization vector  $M$  of the underlying film.<sup>16–18</sup> Experimental evidence has been provided that over a critical angle a propagating spin wave mode can be excited, and below this angle, both localized and propagating spin waves are excited.<sup>19</sup> Madami *et al.* recently observed a propagating spin wave induced by an STT oscillator where they used a Ni<sub>80</sub>Fe<sub>20</sub> (permalloy) film subject to an out-of-plane oriented magnetic field.<sup>20</sup> It is now timely to explore spin-wave propagation velocities and damping of CoFeB in out-of-plane magnetic fields and compare them to permalloy which, so far, is mainly used for magnonic nanodevices and magnonic crystals.<sup>11,22,23</sup> In this paper, we present temperature-dependent measurements on spin wave propagation and damping in CoFeB, applying, both, in in-plane and out-of-plane magnetic fields. We address the temperature range from 5 to 295 K. The intrinsic damping parameter  $\alpha_i$  is found to be as small as 0.007 at 295 K. At the same time, the group velocity is measured to be a factor of about 3 larger compared to permalloy provoking a large decay for CoFeB. The damping parameter is found to increase only below 200 K. We do not observe an in-plane magnetic anisotropy making magnetron-sputtered

CoFeB an interesting material for magnonic devices with electrical spin-wave injection.

Thin films were prepared on semi-insulating GaAs substrates by magnetron sputtering in argon atmosphere using a Co<sub>20</sub>Fe<sub>60</sub>B<sub>20</sub> target.<sup>21</sup> Here, we report data obtained on a 60 nm thick film forming a mesa with an area of 300  $\mu\text{m} \times 120 \mu\text{m}$  as depicted in Fig. 1. A 5 nm thick layer of Al<sub>2</sub>O<sub>3</sub> was grown by atomic layer deposition onto the mesa to ensure an electrical isolation for two shortened metallic coplanar waveguides (CPWs) integrated by optical lithography. These two CPWs were designed to act as a spin wave emitter (CPW1) and detector (CPW2). The six conducting lines were 2  $\mu\text{m}$  wide. The edge-to-edge separation between signal and ground lines was 1.6  $\mu\text{m}$ . The distance  $s$  between the two inner conductors was 12  $\mu\text{m}$ . Reference permalloy (Py) thin films were deposited using electron beam evaporation. The thickness was 40 nm. To measure spin-wave propagation and extract the Gilbert damping parameter  $\alpha_i$ , we connected a vector network analyzer to the CPWs. We measured transmission and reflection signals, respectively.<sup>24</sup> The Fourier analysis of the microwave field generated around the inner conductor of CPW1 provided us with an excitation spectrum<sup>25</sup> which contained two peaks I and II at wave vectors  $k_I$  and  $k_{II}$ , respectively. The wave vectors were perpendicular to the CPW. The magnetic field  $H$  was applied, both, in the film plane and in the out-of-plane direction.

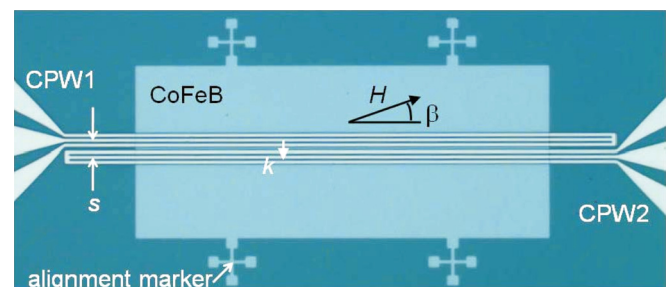


FIG. 1. Microscopy image of a CoFeB mesa with two integrated coplanar waveguides (CPWs). The center-to-center separation  $s$  of the two CPWs is 12  $\mu\text{m}$ . Orientations of in-plane magnetic field  $H$  and wave vector  $k$  are sketched.

<sup>a)</sup>H. Yu and R. Huber contributed equally to this work.

<sup>b)</sup>haiming.yu@ph.tum.de.

<sup>c)</sup>grundler@ph.tum.de.

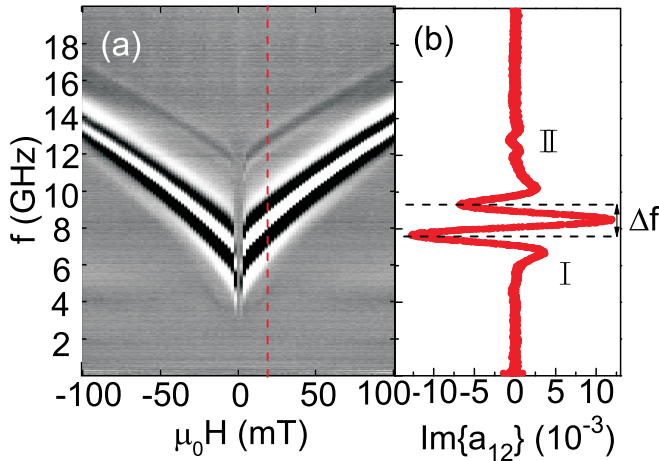


FIG. 2. (a) Gray-scale plot of spectra measured on CoFeB at room temperature in transmission configuration between two neighboring coplanar waveguides. The field is collinear with the CPWs. The dashed line indicates 20 mT where we extract the spectrum shown in (b). The spectrum in (b) is the imaginary part of the transmission signal. The frequency separation denoted by  $\Delta f$  is used to calculate the group velocity. The emitter CPW excites two pronounced modes I and II.

Fig. 2(a) shows color-coded spectra obtained in transmission configuration between emitter and detector CPWs on CoFeB. We depict the imaginary part of the transmission signal.  $\mathbf{H}$  is collinear with the CPWs. We therefore excite Damon-Eshbach-type (DE) modes. We observe two branches which vary characteristically with  $H$ . Each of the modes I and II generates a black-white-black oscillating contrast that indicates spin wave propagation. In Fig. 2(b), we show a single spectrum extracted at 20 mT. Following Refs. 24 and 26, the frequency separation  $\Delta f$  reflects a change in the phase by  $2\pi$  which is accumulated by spin waves propagating between the inner conductors of CPW1 and CPW2. The group velocity  $v_g$  is calculated from  $\Delta f$  according to Ref. 24,

$$v_g = \frac{\partial \omega}{\partial k} \approx \frac{2\pi \Delta f}{2\pi/s} = \Delta f \cdot s. \quad (1)$$

Using Eq. (1), we evaluate group velocities close to the relevant wave vector  $k_1$ . In Fig. 3(a), we summarize the velocities for DE modes in CoFeB as a function of  $H$  (filled circles). At  $\mu_0|H| = 6$  mT, we find 25 km/s. The value

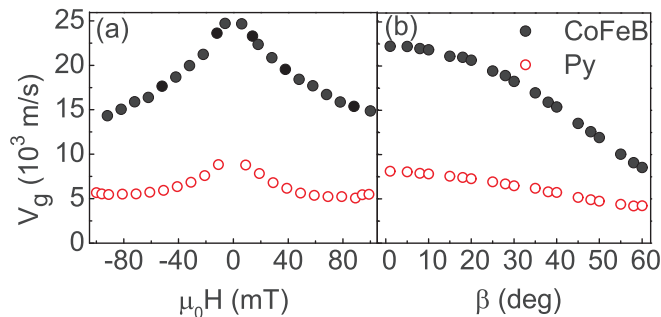


FIG. 3. (a) Group velocities of DE modes at room temperature as a function of applied field. Filled (open) circles denote CoFeB (permalloy). (b) Spin wave group velocity as a function of angle  $\beta$  when the in-plane field amounts to  $\mu_0 H = 20$  mT.

decreases with increasing absolute value of  $\mu_0|H|$ , reaching 15 km/s at 90 mT. Velocities measured on the permalloy reference film (open circles) are found to be a factor of 2.5 to 3 smaller compared to CoFeB. This is attributed mainly to the different values of the saturation magnetization  $M_S$  as will be discussed later.

The excitation spectrum of the emitter CPW consists of two peaks I and II reflecting the wave vectors  $k_I = 0.6 \times 10^4$  rad/cm and  $k_{II} = 2.4 \times 10^4$  rad/cm.<sup>24</sup> This gives rise to the two distinct resonances I and II in the spectra (Fig. 2). From the frequency separation ( $f_{II} - f_I$ ) between two peaks II and I [c.f. Fig. 4(b)], a group velocity can be recalculated according to  $v_g = 2(f_{II} - f_I)/(k_{II} - k_I)$  in an independent way. At 295 K and 20 mT, we obtain 18.6 km/s for CoFeB. This value is slightly smaller compared to 22.3 km/s which we evaluate from Eq. (1) in Fig. 3(b) at 20 mT and  $\beta = 0^\circ$ . The discrepancy can be understood as follow. When using peaks I and II for the evaluation, we average the group velocity over a broad wave vector range ( $k_{II} - k_I$ ). Since the group velocity in general decreases with increasing  $k$ , the value  $2(f_{II} - f_I)/(k_{II} - k_I)$  is expected to be smaller compared to the slope  $v_g = \partial \omega / \partial k = 2\pi \partial f / \partial k$  used in Eq. (1) where we evaluate  $v_g$  close to  $k_1$  only.

When we now fix  $\mu_0|H|$  at 20 mT and rotate the field in the plane of the ferromagnet, the velocity decreases with increasing angle  $\beta$  as shown in Fig. 3(b). Here,  $\beta$  is the angle between  $H$  and the CPW (Fig. 1). For CoFeB (filled circles), the velocity drops from 22.3 to 9.0 km/s when  $\beta$  varies from 0 to  $60^\circ$ . The variation observed for CoFeB is more pronounced compared to permalloy (open circles) where the velocity varies from 8 to 4.5 km/s. We attribute the observed angular dependence of the velocity to the change in angle between the wave vector  $k$  and the magnetization vector  $M$  which follows the rotation of  $H$ . We note that in separate resonance measurements (not shown) where we rotate the sample and keep the angle between  $\mathbf{k}$  and  $\mathbf{H}$  constantly at  $90^\circ$ , we do not observe an in-plane magnetic anisotropy in, both, the polycrystalline magnetron-sputtered CoFeB and evaporated permalloy.

It is now interesting to study the propagation characteristics with the field  $\mathbf{H}$  applied in a direction perpendicular to the plane. When  $\mu_0|H|$  exceeds the shape anisotropy field of CoFeB of about 1.7 T, we obtain transmission spectra such as the one shown in Fig. 4(a). The oscillating signal marked by  $\Delta f$  now reflects propagating magnetostatic forward-

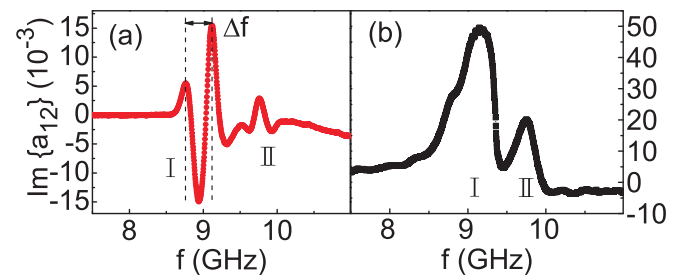


FIG. 4. (a) Imaginary part of the transmission signal obtained on CoFeB when the applied field of 1.9 T is perpendicular to the film plane.  $\Delta f$  indicates the phase shift of  $2\pi$  acquired by the MSFVWs. (b) Imaginary part of the reflection signal with an applied field of 1.9 T being perpendicular to the film plane. Both spectra were measured at 5 K.

volume waves (MSFVWs). The group velocities evaluated between 5 and 295 K are summarized in Fig. 5(a). At 295 K the MSFVW exhibits a velocity of 3.5 km/s. This value is a factor of seven smaller compared to the DE mode. The velocity increases by 25% when cooling down to 5 K, reaching 4.3 km/s. The corresponding values of the permalloy thin film are 1.2 (295 K) and 1.5 km/s (5 K). Again, the velocities measured on permalloy are smaller by about a factor of three.

We measured spectra also in reflection configuration [Fig. 4(b)] to extract information on the linewidth  $\delta f$  and damping in the perpendicular-to-plane field configuration. For this, we fitted a Lorentz curve to mode I and extracted the full width at half maximum as  $\delta f$ . We find  $\delta f$  to increase almost linearly with  $f$  at a given temperature [inset of Fig. 5(b)]. The eigenfrequency  $f$  is varied by changing the magnetic field  $H$ . We analyzed the slope  $\delta f$  vs  $f$  using,<sup>27</sup>

$$\delta f = \frac{|\gamma|}{2\pi} \mu_0 \Delta H + 2\alpha_i f, \quad (2)$$

where  $\gamma$  is the gyromagnetic splitting factor, and  $\Delta H$  reflects a line broadening caused by extrinsic mechanisms and film inhomogeneities. Following Eq. (2), the slope in the inset of Fig. 5(b) provides us with the intrinsic damping parameter  $\alpha_i$ . We have extracted the damping of the CoFeB thin film in perpendicular magnetic fields at different temperatures  $T$  and summarize the values in Fig. 5(b). For  $T \geq 200$  K, we get 0.007 consistent with the earlier reports on CoFeB alloys. Down to 5 K the damping increases by a factor of three to a value of 0.023. We have used the ratio between the signal intensity at the detector and the reflected signal intensity at the emitter  $I_{21}/I_{22}$  to estimate the decay lengths.<sup>24,31</sup> At room

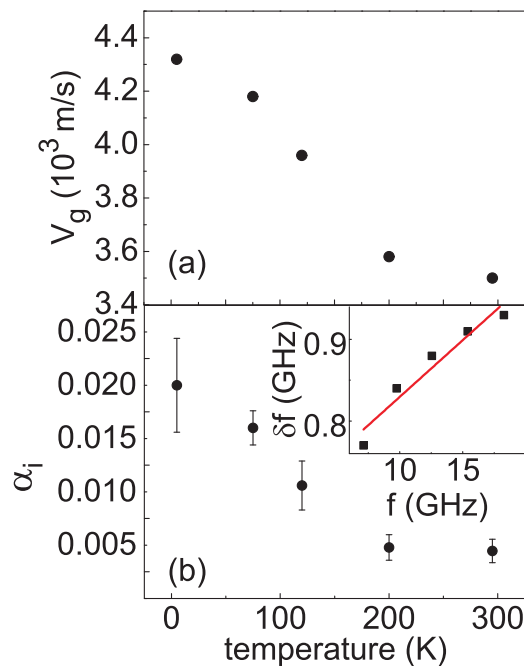


FIG. 5. (a) Group velocity measured on CoFeB in a perpendicular field of 1.9 T at different temperatures  $T$ . The eigenfrequency varies from 5.6 GHz to 7.2 GHz when  $T$  increases from 5 to 295 K. (b) Temperature dependence of intrinsic damping parameter  $\alpha_i$ . The inset shows  $\delta f$  vs  $f(H)$  at 295 K. The line reflects Eq. (2) leading to  $\alpha_i = 0.007$ .

temperature, we obtain a value of 23.9  $\mu\text{m}$  for the DE mode and 4.6  $\mu\text{m}$  for the MSFVW mode in CoFeB.

We now discuss our results. The propagating velocities measured on CoFeB and permalloy are found to differ by about a factor of three. This factor was observed for, both, DE modes and MSFVWs. In the appendix of Ref. 28, group velocities are evaluated for different orientations of  $M$  and  $k$  as a function of film thickness  $d$  and saturation magnetization  $M_S$ . For DE modes, the group velocity reads

$$\frac{1}{v_g} = \frac{4}{\omega_M d} \frac{\sqrt{\omega_0(\omega_0 + \omega_M)}}{\omega_M}. \quad (3)$$

For MSFVW one gets

$$\frac{1}{v_g} = \frac{4}{\omega_M d}. \quad (4)$$

In Eqs. (3) and (4),  $\omega_0 = -\gamma\mu_0 H$ , and  $\omega_M = -\gamma\mu_0 M_S$ . For CoFeB and permalloy, we assume values of  $\mu_0 M_S = 1.8(2)$  T (Ref. 4) and 1.01 T,<sup>29</sup> respectively. Considering DE modes at an applied field of a few 10 mT, the external field is much smaller than the saturation magnetization. In this limit, we obtain  $v_g = \frac{-\gamma\mu_0 d}{4} H^{-\frac{1}{2}} M_S^{\frac{3}{2}}$  from Eq. (3). Starting from a small field  $H$ , the group velocity is expected to decrease with increasing  $H$  according to  $H^{-\frac{1}{2}}$ . This explains why we detect the largest propagation velocities near remanence in Fig. 3(a). Considering the different saturation magnetizations  $M_S$  and thicknesses  $d$ , Eq. (3) predicts group velocities which differ by a factor of  $\frac{d_{\text{CoFeB}} M_{S,\text{CoFeB}}^{3/2}}{d_{\text{Py}} M_{S,\text{Py}}^{3/2}} = 3.4$  between CoFeB and permalloy.<sup>30</sup> This is close to the factor of three observed in Fig. 3(a). For MSFVWs, Eq. (4) predicts  $v_g$  to be 4.8 km/s for CoFeB. We find a value close to this at low temperature in Fig. 5(a).

In general, microscopic origins of spin wave damping include direct and indirect contributions for angular momentum transfer to the lattice.<sup>32</sup> For MSFVW, indirect damping such as two-magnon scattering is suppressed due to the out-of-plane orientation of the magnetization.<sup>28,33</sup> We thus attribute the damping parameter in Fig. 5(b) to direct damping where the spin angular momentum is transferred to non-magnetic degrees of freedom. Processes involved are intra- and inter-band electronic transitions provoked by spin precession in the presence of spin-orbit interaction. Interestingly, we find in Fig. 5(b) that the damping parameter increases below a temperature of about 200 K. Such an increase of  $\alpha_i$  with decreasing temperature has already been observed for further metallic ferromagnets.<sup>34</sup> It is attributed to the variation of the electron scattering time which increases with decreasing  $T$  when electron scattering due to phonons diminishes. A longer electron scattering time favors angular momentum transfer due to direct damping via intra-band transitions.<sup>32</sup> The observed decrease of the damping constant with increasing temperature is consistent with the theoretical work of Gilmore *et al.*,<sup>35</sup> who have used first-principles calculations and discussed damping for ferromagnetic elements such as Fe, Co, and Ni. The observed low damping might be understood by the suppression of spin-flip

transitions which has been reported to occur for half metals and is attributed also to pseudo-gap materials with high spin polarization to which CoFeB alloys belong.<sup>36</sup> A detailed analysis of the resonance peak I in Fig. 4(b) provides that the peak contains a further resonance on the low frequency side. With increasing temperature this additional resonance disappears, providing a Lorentzian-shaped peak at room temperature when the damping is found to be smallest. So far the origin of the additional feature at low  $T$  is not clear.

In conclusion, we have investigated group velocities of spin waves in CoFeB. We obtain values significantly in excess of permalloy which we attribute to the relatively large saturation magnetization of CoFeB. Large decay lengths are to be expected at room temperature as the damping is found to be small and only 0.007.

Financial support by the German Excellence Cluster Nanosystems Initiative Munich (NIM) and the European Community's Seventh Framework Programme (FP7/2007-2013) under Grant Agreement No. 228673 MAGNONICS and the DFG via project GR1640/5-1 in the priority programme SPP1538 is gratefully acknowledged.

- <sup>1</sup>J. S. Moodera, L. R. Kinder, T. M. Wong, and R. Meservey, *Phys. Rev. Lett.* **74**, 3273 (1995).
- <sup>2</sup>S. S. P. Parkin, C. Kaiser, A. Panchula, P. M. Rice, B. Hughes, M. Samant, and S. H. Yang, *Nature Mater.* **3**, 862 (2004).
- <sup>3</sup>S. Ikeda, K. Miura, H. Yamamoto, K. Mizunuma, H. D. Gan, M. Endo, S. Kanai, J. Hayakawa, F. Matsukura, and H. Ohno, *Nature Mater.* **9**, 721 (2010).
- <sup>4</sup>H. Ulrichs, B. Lenk, and M. Münzenberg, *Appl. Phys. Lett.* **97**, 092506 (2010).
- <sup>5</sup>C. Bilzer, T. Devolder, J. V. Kim, G. Counil, C. Chappert, S. Cardoso, and P. P. Freitas, *J. Appl. Phys.* **100**, 053903 (2006).
- <sup>6</sup>G. Malinowski, K. C. Kuiper, R. Lavrijsen, H. J. M. Swagten, and B. Koopmans, *Appl. Phys. Lett.* **98**, 153107 (2011).
- <sup>7</sup>H. Lee, L. Wen, M. Pathak, P. Janssen, P. Leclair, C. Alexander, C. K. A. Mews, and T. Mewes, *J. Phys. D: Appl. Phys.* **41**, 215001 (2008).
- <sup>8</sup>M. Oogane, T. Wakitani, S. Yakata, R. Yilgin, Y. Ando, A. Sakuma, and T. Miyazaki, *Jpn. J. Appl. Phys.* **45**, 3889 (2005).
- <sup>9</sup>X. Liu, W. Z. Matthew, J. Carter, and G. Xiao, *J. Appl. Phys.* **110**, 033910 (2011).
- <sup>10</sup>F. Xu, Q. Huang, Z. Liao, S. Li, Y. Ando, C. K. Ong, and T. Miyazaki, *J. Appl. Phys.* **111**, 07A304 (2012).
- <sup>11</sup>S. Neusser and D. Grundler, *Adv. Mater.* **21**, 2927 (2009).
- <sup>12</sup>V. V. Kruglyak, S. O. Demokritov, and D. Grundler, *J. Phys. D: Appl. Phys.* **43**, 264001 (2010).
- <sup>13</sup>D. C. Worledge, G. Hu, D. W. Abraham, J. Z. Sun, P. L. Trouilloud, J. Nowak, S. Brown, M. C. Gaidis, E. J. OSullivan, and R. P. Robertazzi, *Appl. Phys. Lett.* **98**, 022501 (2011).
- <sup>14</sup>S. I. Kiselev, J. C. Sankey, I. N. Krivorotov, N. C. Emley, R. J. Schoelkopf, R. A. Buhrman, and D. C. Ralph, *Nature* **425**, 380 (2003).
- <sup>15</sup>W. H. Rippard, M. R. Pufall, S. Kaka, S. E. Russek, and T. J. Silva, *Phys. Rev. Lett.* **92**, 027201 (2004).
- <sup>16</sup>G. Gerhart, E. Bankowski, G. A. Melkov, V. S. Tiberkevich, and A. N. Slavin, *Phys. Rev. B* **76**, 024437 (2007).
- <sup>17</sup>G. Consolo, B. Azzèrboni, L. Lopez-Diaz, G. Gerhart, E. Bankowski, V. Tiberkevich, and A. Slavin, *Phys. Rev. B* **78**, 014420 (2008).
- <sup>18</sup>M. A. Silva, T. J. Silva, and M. D. Stiles, *Phys. Rev. B* **77**, 144401 (2008).
- <sup>19</sup>S. Bonetti, V. Tiberkevich, G. Consolo, G. Finocchio, P. Muduli, F. Mancoff, A. Slavin, and J. Åkerman, *Phys. Rev. Lett.* **105**, 217204 (2010).
- <sup>20</sup>M. Madami, S. Bonetti, G. Consolo, S. Tacchi, G. Carlotti, G. Gubbiotti, F. B. Mancoff, and J. Åkerman, *Nature Nanotechnol.* **10**, 1038 (2011).
- <sup>21</sup>Using energy dispersive x-ray analysis of a nominally identical thin film, we find that the composition of the thin film differs from the target composition. For the atomic concentration ratio between Fe and Co, we find 3.6 instead of 3. The exact relative amount of B is not known at this point.
- <sup>22</sup>V. E. Demidov, S. Urazhdin, E. R. J. Edwards, M. D. Stiles, R. D. McMichael, and S. O. Demokritov, *Phys. Rev. Lett.* **107**, 107204 (2011).
- <sup>23</sup>J. Topp, D. Heitmann, and D. Grundler, *Phys. Rev. B* **80**, 174421 (2009).
- <sup>24</sup>S. Neusser, G. Duerr, H. G. Bauer, S. Tacchi, M. Madami, G. Woltersdorf, G. Gubbiotti, C. H. Back, and D. Grundler, *Phys. Rev. Lett.* **105**, 067208 (2010).
- <sup>25</sup>G. E. Ponchak, E. M. Tentzeris, and L. P. B. Katehi, *Int. J. Microcircuits Electron. Packag.* **20**, 167 (1997).
- <sup>26</sup>V. Vlaminck and M. Bailleul, *Science* **322**, 410 (2008).
- <sup>27</sup>B. Kuanr, R. E. Camley, and Z. Celinski, *Appl. Phys. Lett.* **87**(1), 012502 (2005).
- <sup>28</sup>D. D. Stancil and A. Prabhakar, *Spin Waves: Theory and Applications, Appendix C* (Springer, 2009).
- <sup>29</sup>G. Duerr, M. Madami, S. Neusser, S. Tacchi, G. Gubbiotti, G. Carlotti, and D. Grundler, *Appl. Phys. Lett.* **99**, 202502 (2011).
- <sup>30</sup>We consider only the relative factor. Absolute values given by Eq. (3) differ by about a factor of 2 from the measured ones.
- <sup>31</sup>M. Bailleul, D. Olligs, and C. Fermon, *Appl. Phys. Lett.* **83**, 972 (2003).
- <sup>32</sup>M. Fähnle and C. Illg, *J. Phys.: Condens. Matter* **23**, 493201 (2011).
- <sup>33</sup>R. Arias and D. L. Mills, *Phys. Rev. B* **60**, 7395 (1999).
- <sup>34</sup>G. Counil, T. Devolder, J. V. Kim, P. Crozat, C. Chappert, S. Zoll, and R. Fournel, *IEEE Trans. Magn.* **42**, 3323 (2006).
- <sup>35</sup>K. Gilmore, Y. U. Idzerda, and M. D. Stiles, *Phys. Rev. Lett.* **99**, 027204 (2007).
- <sup>36</sup>A. Mann, J. Walowski, M. Münzenberg, S. Maat, M. J. Carey, J. R. Childress, C. Mewes, D. Ebke, V. Drewello, G. Reiss, and A. Thomas, arXiv:1202.3874v1 [cond-mat.mtrl-sci].